Metabolomics Analysis of Tilletia Controversa Kühn Infected and Non-infected Grains of Wheat

Zhaoyu Ren
Chinese Academy of Agricultural Sciences
Ghulam Muhae-Ud-Din
Chinese Academy of Agricultural Sciences
Jianjian Liu
Chinese Academy of Agricultural Sciences
Taiguo Liu
Chinese Academy of Agricultural Sciences
Wanquan Chen
Chinese Academy of Agricultural Sciences
Li Gao (xiagaosx@hotmail.com)
Chinese Academy of Agricultural Sciences

Research Article

Keywords: wheat dwarf bunt, liquid chromatography, mass spectrometry, metabolites, metabolomics, Tilletia controversa

Posted Date: December 10th, 2020

DOI: https://doi.org/10.21203/rs.3.rs-121283/v1

Abstract

Dwarf bunt caused by the pathogen *Tilletia controversa* Kühn is one of the most serious quarantine disease of winter wheat. Metabolomics studies provide detailed information about biochemical changes at the cell and tissue level of the plants. In the present study, liquid chromatography/mass spectrometry (LC/MS) metabolomic approach was used to investigate the changes in the grains metabolomics of *T. controversa* infected and non-infected samples. PCA analysis suggested that *T. controversa* infected and non-infected samples scattered separately during the interaction. LC/MS analysis showed that 62 different metabolites were recorded in the grains, among them total of 34 metabolites were up-regulated and 28 metabolite were down-regulated. The prostaglandins (PGs) and 9-hydroxyoctadecaenoic acids (9-HODEs) are fungal toxin related substances and their expression significantly increased in *T. controversa* infected grains. Additionally, the concentration of cucurbic acid and octadecatrienoic acid were changed significantly after pathogen infection, which has great role in plant defense. The eight different metabolic pathways activated during the *T. controversa* and wheat plants interactions including phenylalanine metabolism, isoquinoline alkaloid biosynthesis, starch and sucrose metabolism, tyrosine metabolism, sphingolipid metabolism, arginine and proline metabolism, alanine, aspartate, glutamate metabolism, and tryptophan metabolism.

Introduction

Wheat is one of the most important staple crops and plays a fundamental role in food security worldwide [1]. Wheat production was often negatively affected by the infection of a wide variety of pathogens. Wheat dwarf bunt (caused by a fungal pathogen *Tilletia controversa* Kühn) is a destructive disease which causes significant quality and quantity losses in wheat growing regimes [2]. Metabolomics is an omics technology for comprehensive evaluation of small, endogenous molecules (such as nucleotides, organic acids, sugar and amino acids) which helps to analyse the interrelationships between genetic structure, gene expression, protein function, and environmental impact [3]. These compounds are the substrates and by-products of cell processes (such as enzymatic reactions) and, as such have a direct effect on phenotypes. The sub-discipline of plant metabolomics is a growing research in the plant-microbe interaction area [4,5]. Plant defense mechanisms can be regulated by metabolomics in fungus-infected plants. When plant infected by the pathogen, the plant activates a multi-component biochemical and physical response involving radical changes in the expression patterns of proteins, genes and metabolites [6,7]. Metabolites are the end products of translation and transcription; therefore, the changes in metabolites abundance may be regarded as a major feature of plant interactions with pathogen and environment [3,8] Previous studies showed that wheat metabolites were different in *F. graminearum* infected and normal plants [9]. *Magnaporthe oryzae* altered the alanine contents in rice compared to normal rice leaves [10]. Doehleman [11] investigated the metabolites in maize tumor after *U. maydis* infection. Similarly, metabolic profiling strategies were used to determine the mechanisms of plant defense against *R. solani* in soybean, rice, lettuce, and potato [12–15]. Metabolomics analysis have been performed in *B. cinerea* infected tomato, strawberry, *Arabidopsis* and grapes [16,17]. GC-MS based

metabolomics approach was done on the *S. sclerotiorum* infected susceptible and resistance cultivars of soybean. Results of this study showed that antifungal activity increased in the resistant cultivar by reprograming the phenylpropanoid pathway [18]. Similarly, untreated LC-MS metabolomics strategy was performed to investigate metabolome alterations in the anthracnose causing *C. sublineolum* [19,20]. Additionally, GC-ESI-MS/MS technique was used in wheat crop infected by *S. nodorum* and found that the concentration of secondary metabolites was 200 higher in the mutants strain compared to wide [21]. Metabolomics studies are very useful in plant sciences because it offers the ability to recognise biochemical alterations relatively quickly, usually before any change in the phenotypes of crops [10].

Plant-pathogen relationships are extremely interesting in terms of both biological importance and metabolite richness and thus an ideal area for exploration using metabolomics techniques [10]. Liquid chromatography-mass spectrometry (LC-MS) is a sensitive tool for metabolic profiling that perfectly compensates for this defect and has become an important research method in the field of metabolomics [22,23]. LC-MS-based analysis aims to compare multiple biological groups to detect metabolites that have changed significantly after pathogen infection. In the present work LC-MS technique was used to study the response of metabolites in *T. controversa* infected grains (galls) and normal grains. Clear differences were obtained in metabolic profiles of wheat grains after *T. controversa* infection. According to our knowledge, it is the first study to evaluate the metabolites in wheat grains after *T. controversa*.

Materials And Methods

2.1. Plant material and pathogen inoculation

Wheat (*Triticum aestivum* L) cv Dongxuan 3 seeds were collected from Institute of Plant Protection, Chinese Academy of Agricultural Sciences, Beijing-China. Wheat seeds were sterilized with 30% sodium hypochlorite for 5 min, rinsed 5 times in water, and germinated for 30 days in incubator (AUCMA, Qing Dao, China) to vernalize. After vernalization, seedlings were grown in a 1:2 mixture of organic matter (peat moss, Beijing, China) and soil (Beijing, China) in pots. The pots were kept in incubator (AUCMA, Qing Dao, China) under a 14 h light: 10 h dark (8–10 ˚C, 70% humidity) regime and temperature was increased to 20 ˚C during boot stage. The pathogenic fungus *T. controversa* Kühn was gifted by Blair Goates (the United States Department of Agriculture (USDA), Agricultural Research Service (ARS), Aberdeen, Idaho, USA). *T. controversa* was propagated in soil agar medium (20 g agar powder, 75 g soil in one liter distilled water) and autoclaved for pouring the media into sterilized plates. After pouring, the plates were incubated at 5 °C in a 24 h light in incubator (MLR 352H, Panasonic, USA) after covering with parafilm for 60 days incubation. Mycelium production were observed under an automated invert fluorescence microscope (IX83, Olympus, Japan). Hyphae were collected with distilled water and used to inoculate wheat plants. During the boot stage, hyphae was injected into spike with the syringe. The hyphae was inoculated twice a day (5 mL per spike) and consecutively for 5 days, while only ddH_2O was used for control plants. The pathogen infected grains (galls) and normal grains was harvested and

quickly dipped in liquid nitrogen and stored at -80 ˚ C for further use. Nine replications of each treatment was used for reproducibility.

2. 2. Sample Processing

Metabolites were extracted from a 50 mg of crushed grains using ultrapure (Watsons, China) water. The choice of extraction method is an important factor in any metabolomics study. The grains were crushed by following the developed method of our laboratory. Briefly, two-three grains were dipped into 2 ml Eppendorf tube containing sterilized steel ball (1.5 mm) with appropriate amount of steel balls and grinded in grinder machine (FastPrep 24 5G, MP Biomedicals, USA) for l minute at 70 Hz for crushing. Every sample grinded 3 times for better results. Powdered tissue sample (50 mg) were first mixed with 500 µl of a ultrapure water (1:10 w/V) and sonicated for 10 min. After this time, 50 µl was taken from homogenate mixture and added into 450 µl of precipitant containing internal standard (methanol: acetonitrile = 1:1). The samples were then vortex for 1 min, centrifuging at 13000 rpm for 10 min. The finally resultant product (100 µL) was then transferred to separate new sterilized Eppendorf tubes for LC-MS analysis.

2.3. LC-MS analysis

LC-MS analysis of the precipitant was done in 450 µl of a methanol- acetonitrile mix. Analysis was done using a liquid chromatograph mass spectrometry (Dionex ultimate 3000, Thermo Fisher) with a C18 column (2.1 × 100 mm, 3 µm particle size, Waters). After a 5 µl of sample injection chromatographic analysis was achieved with a liquid phase of 2 mmol / L ammonium acetate and 0.1% formic acid in water (A) and acetonitrile (D). The detailed gradient elution program was shown as followed, 95% (A) and 5% (D) to 0–2 min; 5% (A) and 95% (D) to 42–47 min; 95% (A) and 5% (B) to 47.10–50 min.

Mass spectrometry (MS) was performed in positive electrospray ionization mode (ESI +). The instrument parameters were optimized as follows: ion spray voltage, 3000V; evaporation temperature, 350 ˚C; sheath gas, 35Arb; auxiliary gas, 10Arb; capillary temperature, 320 ˚C. The compound spectrometry parameters were optimized as follows: resolution, 70000; AGC target, 1e6; maximum TT, 100 ms; scanning range, 100-1500m / Z.

2.4. Data processing

All LC-MS dates were further filtered by using the R platform loaded with the xcms tool kit including; peak matching, retention time correction, variable integration and data standardization. The preprocessed data was then analysed by multivariate analysis, including principal components analysis (PCA) and orthogonal partial least squares discriminant analysis (OPLS-DA) by EZinfo software, and hierarchical cluster analysis (HCA) was performed by MetaboAnalyst 4.0 software. Metabolic pathways were further analyzed using KEGG (http://www.genome.jp/kegg/). The correlation analysis of differential metabolites was calculated by using R software and Cytoscape software was used for network construction.

Results

3.1. Metabolite identification- LC-MS

The chromatogram of the positive ions and negative ions of wheat grains extract respectively. The total ion concentration of positive ions (Fig. 1a) and negative ions (Fig. 1b) demonstrated with different time intervals using high-resolution mass spectrometry in different time intervals. The peak of positive and negative ions was obtained within 25–30 minutes (time interval) during analysis. The qualitative relative abundance of aspartic and its molecular obtained by using LC-MS (Fig. 1 **cd**). Additionally, all metabolite was found and their statistical significance were demonstrated in Table 1.

Table 1
List of identified metabolites from *T. controversa* infected and non-infected wheat grains

Metabolite	VIP-value	TCK Vs. CK (%)	Metabolite	VIP-value	TCK Vs.CK (%)
Octadecatrienoic acid	12.679 *	769.59 ↑	L-Valine	10.858 *	36.71 ↓
L-Glutamine	7.2423 *	403.43 ↑	9,12,13-TriHOME	6.4916 *	85.55 ↓
Dodecanoylcarnitine	6.438 *	5430.78 ↑	Malic acid	6.2193 *	57.64 ↓
Clupanodonic acid	5.1969 *	912.54 ↑	Pidolic acid	4.9952 *	400.71 ↑
9-HODE	4.3995 *	274.41 ↑	Androsterone	3.1927 *	20255.36 ↑
Succinylcholine	3.1339 *	20616.86 ↑	Glycerophosphocholine	3.103 *	499.13 ↑
Nervonic acid	2.9982 *	68488.93 ↑	L-Arginine	2.7727 *	691.73 ↑
O-beta-glucoside	2.7681 *	35.23↓	D-Sorbitol	2.7338 *	4745.88 ↑
Maokonine	2.7103 *	99.51 ↓	Caffeic acid	2.6764 *	46839.69 ↑
L-Proline	2.6358 *	66.43 ↓	Allysine	2.3258 *	27.34 ↓
L-Leucine	2.2687 *	240.34 ↑	Hydroxymethylproline	2.2432 *	33.56 ↓
Alloisoleucine	2.2421 *	239.04 ↑	Pyroglutamic acid	2.2176 *	1503.26 ↑
D-Glucose	2.2036 *	73.29 ↓	Nicotinamide	2.1041 *	20.77 ↓
Sphinganine	1.9169 *	104.08 ↑	L-Asparagine	1.8431 *	395.53 ↑
Phenyl pyruvic acid	1.7164 *	2365.69 ↑	D-Arabitol	1.6904 *	2093.50 ↑
Adenine	1.6198 *	130.52 ↑	Cuscohygrine	1.6038 *	96.35 ↓

↑ indicates the up-regulation and ↓ indicate the down-regulation of the metabolite. VIP ≥ 1 stands for significant and * showed the significant of the respective metabolite. TCK Vs. CK (%) more than 100 stands for up-regulation (↑) and less than 100 stands for down-regulation ↓. Variable importance for the projection (VIP) > 1 stands for the level of significant. * demonstrate about significance

Metabolite	VIP-value	TCK Vs. CK (%)	Metabolite	VIP-value	TCK Vs.CK (%)
Fumaric acid	1.5928 *	52.84 ↓	L-Phenylalanine	1.5695 *	294.57 ↑
L-Histidine	1.552 *	360.28 ↑	Phenylalanine	1.5408 *	289.86 ↑
Aminobenzoic acid	1.5355 *	327.45 ↑	Aminoisobutyric acid	1.4955 *	72.28 ↓
Aminobutanoic acid	1.4917 *	71.96 ↓	Cellobiose	1.4844 *	4.00 ↓
Cucurbic acid	1.4785 *	68.42 ↓	L-Carnitine	1.3931 *	1086.24 ↑
Coronaric acid	1.3284 *	345.93 ↑	Tetracosanoic acid	1.327 *	3430.50 ↑
Maltol	1.3163 *	19.42 ↓	γ- Guanidinobutyric acid	1.2612 *	47.15 ↓
10-Gingediol	1.2581 *	32.89 ↓	4-Guanidinobutanoic acid	1.2481 *	47.21 ↓
3-Hydroxyproline	1.2312 *	90.77 ↓	Tetradecanoylcarnitine	1.2295 *	3188.50 ↑
γ-L-Glutamyl-glutamine	1.2055 *	492.89 ↑	Adenosine	1.2029 *	56.74 ↓
Neuraminic acid	1.1986 *	56.64 ↓	L-Tyrosine	1.1736 *	341.11 ↑
L-Lysine	1.1325 *	423.06 ↑	Prostaglandin D3	1.1192 *	459.95 ↑
Azelaic acid	1.0857 *	37.86 ↓	Palmitic acid	1.0643 *	18.20 ↓
L-Tryptophan	1.0639 *	203.38 ↑	Pregabalin	1.0448 *	0.54 ↓
10-Gingerol	1.0388 *	52.27 ↓	Stearic acid	1.0246 *	22.51 ↓

↑ indicates the up-regulation and ↓ indicate the down-regulation of the metabolite. VIP ≥ 1 stands for significant and * showed the significant of the respective metabolite. TCK Vs. CK (%) more than 100 stands for up-regulation (↑) and less than 100 stands for down-regulation ↓. Variable importance for the projection (VIP) > 1 stands for the level of significant. * demonstrate about significance

3.2. PCA analysis of T. controversa infected and control samples

Principle component analysis score plot exhibited good clustering between *T. controversa* infected and non-infected samples. Results showed that the distribution of *T. controversa* infected and non-infected metabolites in these two groups was significantly different (Fig. 2a). OPLS-DA plot revealed that the samples of *T. controversa* was mainly distributed on the right side and non-infected samples distributed left side (Fig. 2b). Receiver operating characteristic (ROC) curve was generated by using Monte Carlo cross validation (MCCV) under balanced sub sampling. In each MCCV, two-thirds of the samples was used to assess the importance of features. Results showed that metabolites successfully detected under ROC curve (**Fig. S1**). The list of metabolites and their significant difference on the base of VIP value demonstrated in Table 1. According to results presented in Table 1 and in Fig. 2b, 62 differential metabolites were screened. Out of the 62 metabolites, 34 were up-regulated and 28 were down-regulated. Out of 34 up-regulated metabolites, 12 related to amino acids, 10 organic acids, 3 alcohols, 1 nucleoside and 8 other classes were identified. Similarly, out of 25 down-regulated metabolites, 5 related to amino acids, 10 organic acids, 2 fatty acids, 1 alcohol, 3 sugar, 1 nucleoside and 6 other metabolites. All up-regulated and down-regulated metabolites illustrated in Table 1.

3.3. Screening and statistical analysis of differential metabolites

The correlation between *T. controversa* infected and non-infected samples demonstrated in Fig. 3a. Red color indicates the positive correlation while blue color indicates the negative correlation. Results showed that metabolites in the same branch along horizontal axis had strongest positive correlation. Additionally, metabolites among the control and infected grain groups were seen in the hierarchical clustering analysis (Fig. 3b).

3.4. Metabolic pathways analysis

Influence coefficient of the metabolic pathways, the pathway with the impact value higher than 0.1 was found to be a potential target pathway. As a result, phenylalanine metabolism, isoquinoline alkaloid biosynthesis, starch and sucrose metabolism, tyrosine metabolism, sphingolipid metabolism, arginine and proline metabolism, alanine, aspartate and glutamate metabolism and tryptophan metabolism were closely related pathways in this study (Table 2 **and** Fig. 4).

Table 2
List of metabolic pathways activated in the grains of *T. controversa* infected and non-infected.

Metabolic pathways	Total	Hits	FDR	Impact
Phenylalanine metabolism	12	2	0.0608	0.7221
Isoquinoline alkaloid biosynthesis	6	1	0.1888	1.0000
Starch and sucrose metabolism	22	1	0.5378	1.0000
Tyrosine metabolism	18	2	0.1239	1.0000
Sphingolipid metabolism	17	1	0.4486	1.0000
Arginine and proline metabolism	28	4	0.0135	0.4274
Alanine, aspartate and glutamate metabolism	22	3	0.0367	0.4975
Tryptophan metabolism	23	1	0.5539	1.0000

Discussion

Wheat is one of the major staple food crops worldwide. Wheat crops have evolved efficient mechanisms to inhibit the negative effects of pathogen attack [24]. The critical differences between plants that become diseased or remain healthy after pathogen infection is the recognition of elicitors molecules released by the pathogens [25,26]. The earliest response in plants after pathogen infection is due to the oxidative burst that can triggered hypersensitive cell death. This is celled the hypersensitive response (HR) and is one of the basic cellular response following successful pathogen recognition in plants and a major element of plant disease resistance [27]. Therefore, any change in the primary and secondary metabolites of plants in response to pathogen infection may thus be the key difference in the successful defence against pathogen.

Proline is a multi-functional amino acid which confer resistance against plant pathogens [28,29] and abiotic factors [30,31]. Resistance plants increase the proline accumulation against pathogen infections and vice versa in the susceptible plants [28]. Similarly, cucurbic acid, a compound similar to JA molecule actively involved in the defense mechanisms and tuberization in different crops [32]. Our results showed the concentration of proline, hydroxyproline, hydroxymethylproline and cucurbic acid decreased after *T. controversa* infection (Table 1). The decreasing of the proline contents is the common reaction and energy demand increase for cross-signaling in plant pathogen interaction. It is also possible that elicitor molecules here not recognized by susceptible plants thus cause decrease in proline and cucurbic level, which can facilitate the pathogen infection. Prostaglandin molecule act in multi-dimensional manner in the fungi, but its biological function in the metabolism of fungi still unclear [33,34]. However, the impact of prostaglandin on fungal pathogenesis is still not well clear, but the concentration of prostaglandin increased during the pathogen infection, which has resemblance with our results (Table 1). Prostaglandin

used as signal molecule to induce pathogen infection [35]. Previous study reveals that the silenced of triple-*ppo* (gene have role in prostaglandin production) mutant of *Aspergillus fumigatus* was more virulent comparing to *A. fumigatus* wild-type in the infected murine test model. The *A. fumigatus* mutant showed higher resistance compared to *A. fumigatus* wild against reactive-oxygen species (ROS) produced by the plants for strong defense system after *A. fumigatus* infection [34]. Additionally, prostaglandin have role to increase other fungal metabolite including tyrosine, phenylalanine and other secondary metabolites [36,37]. The 9-hydroxyoctadecaenoic acids (9-HODEs) molecules are oxidation products of linoleic acid molecules that have role in the defense mechanism and increased plant growth as well as promote aflatoxin B1 in *Aspergillus parasiticus* and sterigmatocystin (ST) from *Aspergillus nidulans* [38–40]. The 9-HODEs also act as a quorum sensing signal molecule to regulate the development and growth of *Aspergillus ochraceus* [41]. Our results showed that during *T. controversa* and wheat interactions the concentration of 9-HODE molecule significantly increased suggest that *T. controversa* effects the wheat grains.

An important and preliminary character of metabolomics data is that it can measure a huge number of metabolites in a quantitatively trustworthy way and therefore allows for discovery of correlations between pair of metabolites, even when biological connection between them are not clear. In our results, the metabolites from the grains, little strong correlation was noted. However, for some metabolites there was a positive or negative correlation in the heatmap analysis (**Fig. 3ab**). Additionally, the relative abundance of pathogen infected and control groups scattered separately, which may suggest that grains metabolites infected by the *T. controversa*. For example, the metabolites that are decreased or increase after pathogen infection are involved in the energy metabolism. These changes in the plant metabolites may be the result of *T. controversa* infection.

Declarations

Author contributions

LG conceived the experiment work, ZR performed the experiment analysis, GM drafted the experiment, JL,TL and WC revised critically the manuscript.

Declaration of competing interest

Authors declare that there is no competing interest between them

References

1. Zhang, Z. *et al.* An R2R3 MYB transcription factor in wheat, Ta PIMP 1, mediates host resistance to *Bipolaris sorokiniana* and drought stresses through regulation of defense-and stress-related genes. *New Phytol.***196**, 1155–1170 (2012).

2. Chen, J. *et al.* A novel QTL associated with dwarf bunt resistance in Idaho 444 winter wheat. *Theor. Appl. Genet.***129**, 2313–2322 (2016).
3. Fiehn, O. Metabolomics - The link between genotypes and phenotypes. *Plant Mol. Biol.***48**, 155–171 (2002).
4. Heuberger, A. L., Robison, F. M., Lyons, S. M. A., Broeckling, C. D. & Prenni, J. E. Evaluating plant immunity using mass spectrometry-based metabolomics workflows. *Front. Plant Sci.***5**, 291 (2014).
5. Nielsen, K. F. & Larsen, T. O. The importance of mass spectrometric dereplication in fungal secondary metabolite analysis. *Front. Microbiol.***6**, 71 (2015).
6. Scheel, D. Resistance response physiology and signal transduction. *Curr. Opin. Plant Biol.***1**, 305–310 (1998).
7. Somssica, I. E. & Hahlbrock, K. Pathogen defence in plants - A paradigm of biological complexity. *Trends Plant Sci.***3**, 86–90 (1998).
8. Fiehn, O., Kopka, J., Trethewey, R. N. & Willmitzer, L. Identification of uncommon plant metabolites based on calculation of elemental compositions using gas chromatography and quadrupole mass spectrometry. *Anal. Chem.***72**, 3573–3580 (2000).
9. Lowe, R. G. T. *et al.* A Combined 1H nuclear magnetic resonance and electrospray ionization-mass spectrometry analysis to understand the basal metabolismof plant-pathogenic *Fusarium* spp. *Mol. Plant-Microbe Interact.***23**, 1605–1618 (2010).
10. Jones, O. A. H. *et al.* Using metabolic profiling to assess plant-pathogen interactions: An example using rice (*Oryza sativa*) and the blast pathogen Magnaporthe grisea. *Eur. J. Plant Pathol.***129**, 539–554 (2011).
11. Doehlemann, G. *et al.* Reprogramming a maize plant: Transcriptional and metabolic changes induced by the fungal biotroph *Ustilago maydis*. *Plant J.***56**, 181–195 (2008).
12. Verwaaijen, B. *et al.* A comprehensive analysis of the *Lactuca sativa*, L. transcriptome during different stages of the compatible interaction with *Rhizoctonia solani*. *Sci. Rep.***9**, 7221 (2019).
13. Aliferis, K. A., Faubert, D. & Jabaji, S. A metabolic profiling strategy for the dissection of plant defense against fungal pathogens. *PLoS One***9**, e111930 (2014).
14. Copley, T. R., Aliferis, K. A., Kliebenstein, D. J. & Jabaji, S. H. An integrated RNAseq-1H NMR metabolomics approach to understand soybean primary metabolism regulation in response to Rhizoctonia foliar blight disease. *BMC Plant Biol.***17**, 84 (2017).
15. Ghosh, S., Kanwar, P. & Jha, G. Alterations in rice chloroplast integrity, photosynthesis and metabolome associated with pathogenesis of *Rhizoctonia solani*. *Sci. Rep.***7**, 41610 (2017).
16. Camañes, G., Scalschi, L., Vicedo, B., González-Bosch, C. & García-Agustín, P. An untargeted global metabolomic analysis reveals the biochemical changes underlying basal resistance and priming in *Solanum lycopersicum*, and identifies 1-methyltryptophan as a metabolite involved in plant responses to *Botrytis cinerea* and *Pseudomonas syringae*. *Plant J.***84**, 125–139 (2015).

17. Lloyd, A. J. *et al.* Metabolomic approaches reveal that cell wall modifications play a major role in ethylene-mediated resistance against *Botrytis cinerea*. *Plant J.***67**, 852–868 (2011).
18. Robison, F. M. *et al.* Common bean varieties demonstrate differential physiological and metabolic responses to the pathogenic fungus *Sclerotinia sclerotiorum*. *Plant Cell Environ.***41**, 2141–2154 (2018).
19. Tugizimana, F., Djami-Tchatchou, A. T., Steenkamp, P. A., Piater, L. A. & Dubery, I. A. Metabolomic analysis of defense-related reprogramming in sorghum bicolor in response to *Colletotrichum sublineolum* infection reveals a functional metabolic web of phenylpropanoid and flavonoid pathways. *Front. Plant Sci.***9**, 1840 (2019).
20. Tugizimana, F. *et al.* Time-resolved decoding of metabolic signatures of in vitro growth of the hemibiotrophic pathogen *Colletotrichum sublineolum*. *Sci. Rep.***9**, 3290 (2019).
21. Tan, K. C., Trengove, R. D., Maker, G. L., Oliver, R. P. & Solomon, P. S. Metabolite profiling identifies the mycotoxin alternariol in the pathogen *Stagonospora nodorum*. *Metabolomics***5**, 330–335 (2009).
22. Theodoridis, G. A., Gika, H. G., Want, E. J. & Wilson, I. D. Liquid chromatography-mass spectrometry based global metabolite profiling: A review. *Anal. Chim. Acta***711**, 7–16 (2012).
23. Gika, H. G., Theodoridis, G. A., Plumb, R. S. & Wilson, I. D. Current practice of liquid chromatography-mass spectrometry in metabolomics and metabonomics. *J. Pharm. Biomed. Anal.***87**, 12–25 (2014).
24. Chen, Y. *et al.* Wheat microbiome bacteria can reduce virulence of a plant pathogenic fungus by altering histone acetylation. *Nat. Commun.***9**, 1–14 (2018) doi:10.1038/s41467-018-05683-7.
25. Del Pozo, O., Pedley, K. F. & Martin, G. B. MAPKKKα is a positive regulator of cell death associated with both plant immunity and disease. *EMBO J.***23**, 3072–3082 (2004).
26. Pedley, K. F. & Martin, G. B. Identification of MAPKs and their possible MAPK kinase activators involved in the pto-mediated defense response of tomato. *J. Biol. Chem.***279**, 49229–49235 (2004).
27. Govrin, E. M. & Levine, A. The hypersensitive response facilitates plant infection by the necrotrophic pathogen *Botrytis cinerea*. *Curr. Biol.***10**, 751–757 (2000).
28. Fabro, G., Kovács, I., Pavet, V., Szabados, L. & Alvarez, M. E. Proline accumulation and AtP5CS2 gene activation are induced by plant-pathogen incompatible interactions in Arabidopsis. *Mol. Plant-Microbe Interact.***17**, 343–350 (2004).
29. Cecchini, N. M., Monteoliva, M. I. & Alvarez, M. E. Proline dehydrogenase contributes to pathogen defense in Arabidopsis. *Plant Physiol.***155**, 1947–1959 (2011).
30. Lehmann, S., Funck, D., Szabados, L. & Rentsch, D. Proline metabolism and transport in plant development. *Amino Acids***39**, 949–962 (2010).
31. Szabados, L. & Savouré, A. Proline: a multifunctional amino acid. *Trends Plant Sci.***15**, 89–97 (2010).
32. Honda, I., Seto, H., Turuspekov, Y., Watanabe, Y. & Yoshida, S. Inhibitory effects of jasmonic acid and its analogues on barley (*Hordeum vulgare* L.) anther extrusion. *Plant Growth Regul.***48**, 201–206 (2006).

33. Noverr, M. C. & Huffnagle, G. B. Regulation of Candida albicans morphogenesis by fatty acid metabolites. *Infect. Immun.***72**, 6206–6210 (2004).
34. Tsitsigiannis, D. I. *et al.* Aspergillus cyclooxygenase-like enzymes are associated with prostaglandin production and virulence. *Infect. Immun.***73**, 4548–4559 (2005).
35. Serhan, C. N. Pro-resolving lipid mediators are leads for resolution physiology. **510**, 92-101 (2014) doi:10.1038/nature13479.
36. Chandrasekar, P. H. & Manavathu, E. K. Do Aspergillus species produce biofilm? *Future Microbiol.***3**, 19–21 (2008).
37. Dague, E., Alsteens, D., Latgé, J. P. & Dufrêne, Y. F. High-resolution cell surface dynamics of germinating *Aspergillus fumigatus* conidia. *Biophys. J.***94**, 656–660 (2008).
38. Yan, S., Liang, Y., Zhang, J., Chen, Z. & Liu, C. M. Autoxidated linolenic acid inhibits aflatoxin biosynthesis in *Aspergillus flavus* via oxylipin species. *Fungal Genet. Biol.***81**, 229–237 (2014).
39. Burow, G. B., Nesbitt, T. C., Dunlap, J. & Keller, N. P. Seed lipoxygenase products modulate Aspergillus mycotoxin biosynthesis. *Mol. Plant-Microbe Interact.***10**, 380–387 (1997).
40. Hamberg, M., Sanz, A. & Castresana, C. Alpha-oxidation of fatty acids in higher Plants. *J. Biol. Chem.***274**, 24503–24513 (1999).
41. Gao J, L. Z. Effect of oxylipins on ochratoxin A production by Aspergillus ochraceus in soybean culture medium. *Microbiol. Bull.***47**, 1721–1729 (2020).

Figures

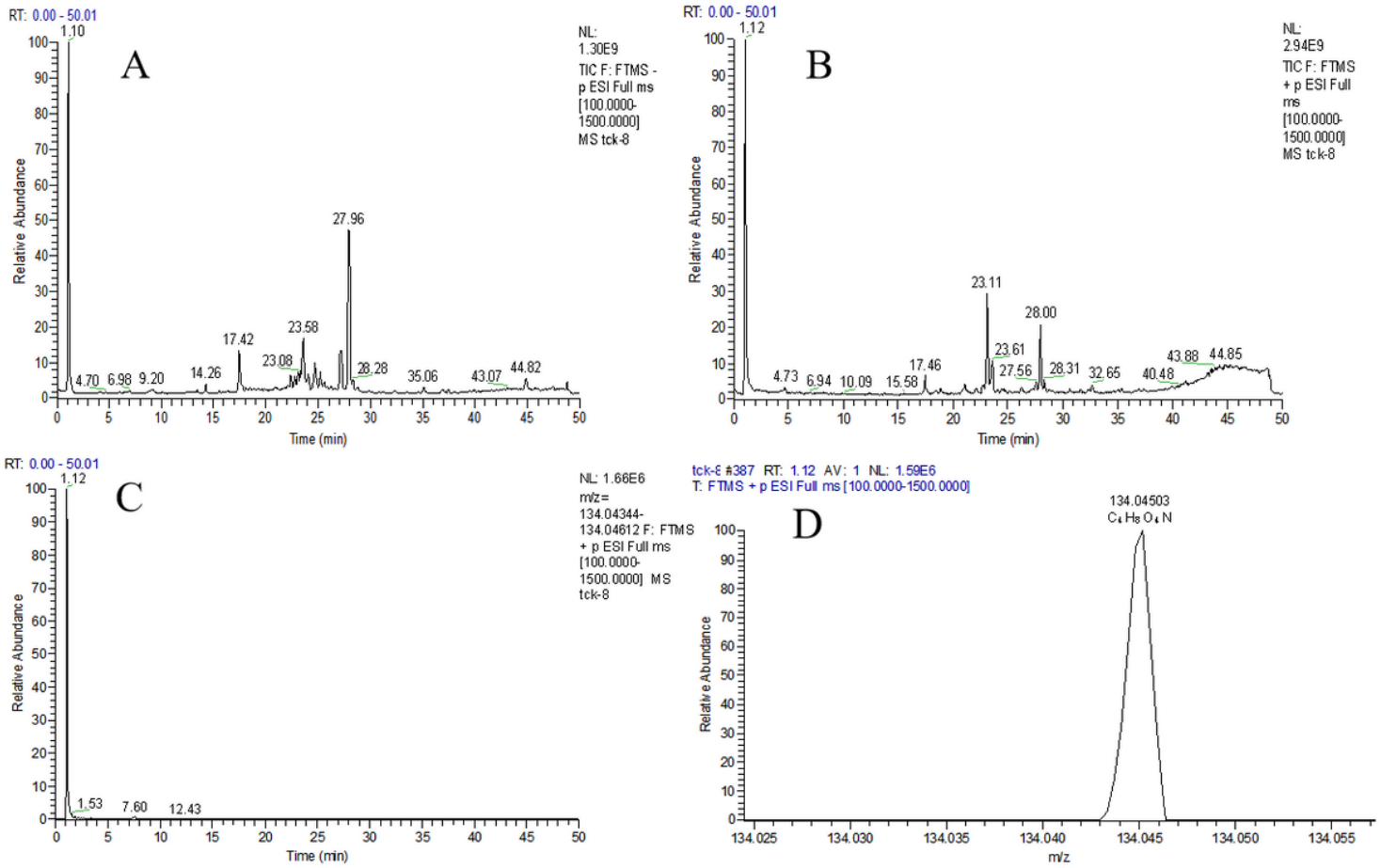

Figure 1

GC-MS chromatograms of the wheat grains metabolites (X-axis= time and Y-axis=response. a relative abundance of positive ions in different time of intervals. b relative abundance of negative ions in different time of intervals. c relative abundance of aspartic acid in different time of intervals. d chemical formula of aspartic acid.

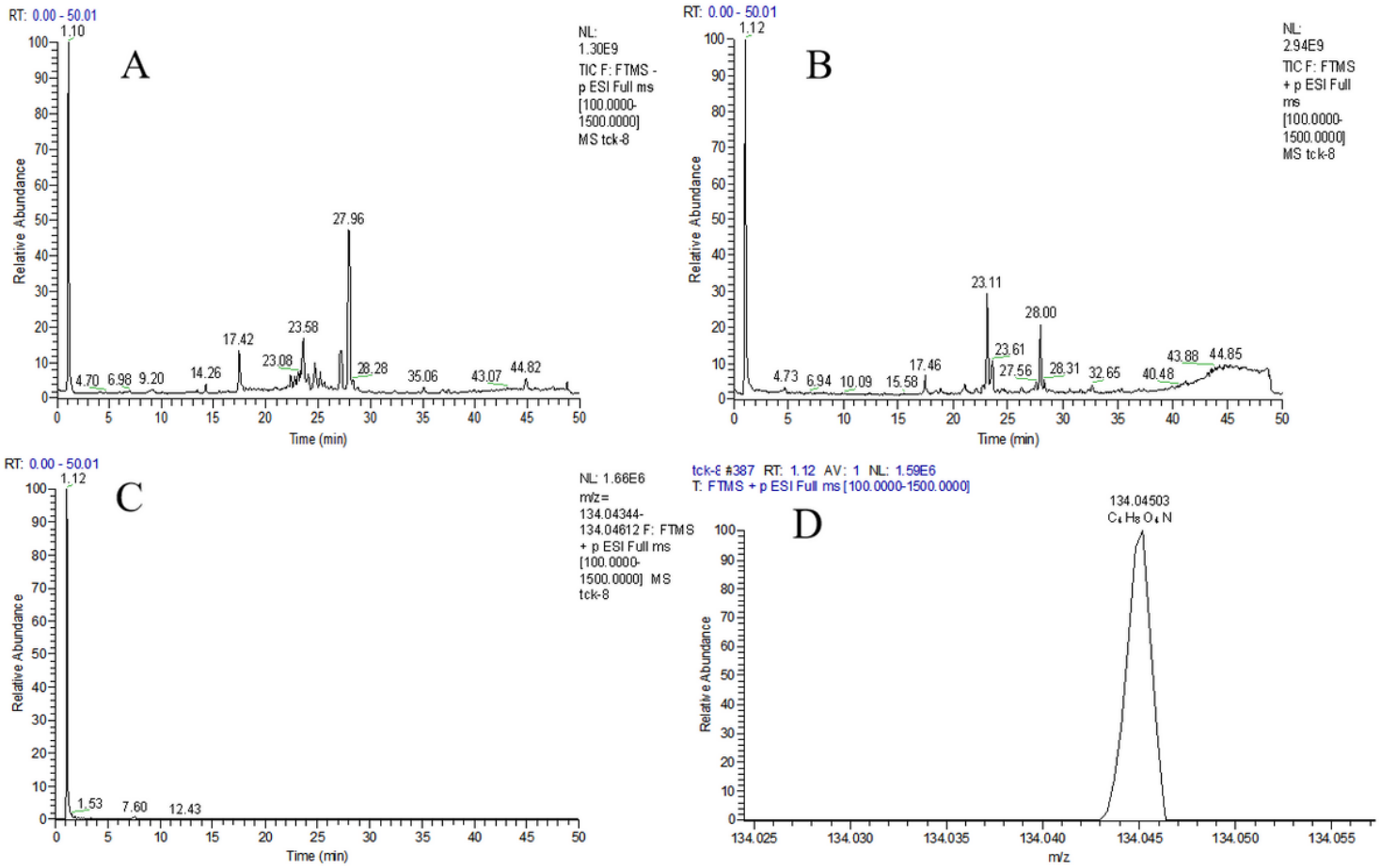

Figure 1

GC-MS chromatograms of the wheat grains metabolites (X-axis= time and Y-axis=response. a relative abundance of positive ions in different time of intervals. b relative abundance of negative ions in different time of intervals. c relative abundance of aspartic acid in different time of intervals. d chemical formula of aspartic acid.

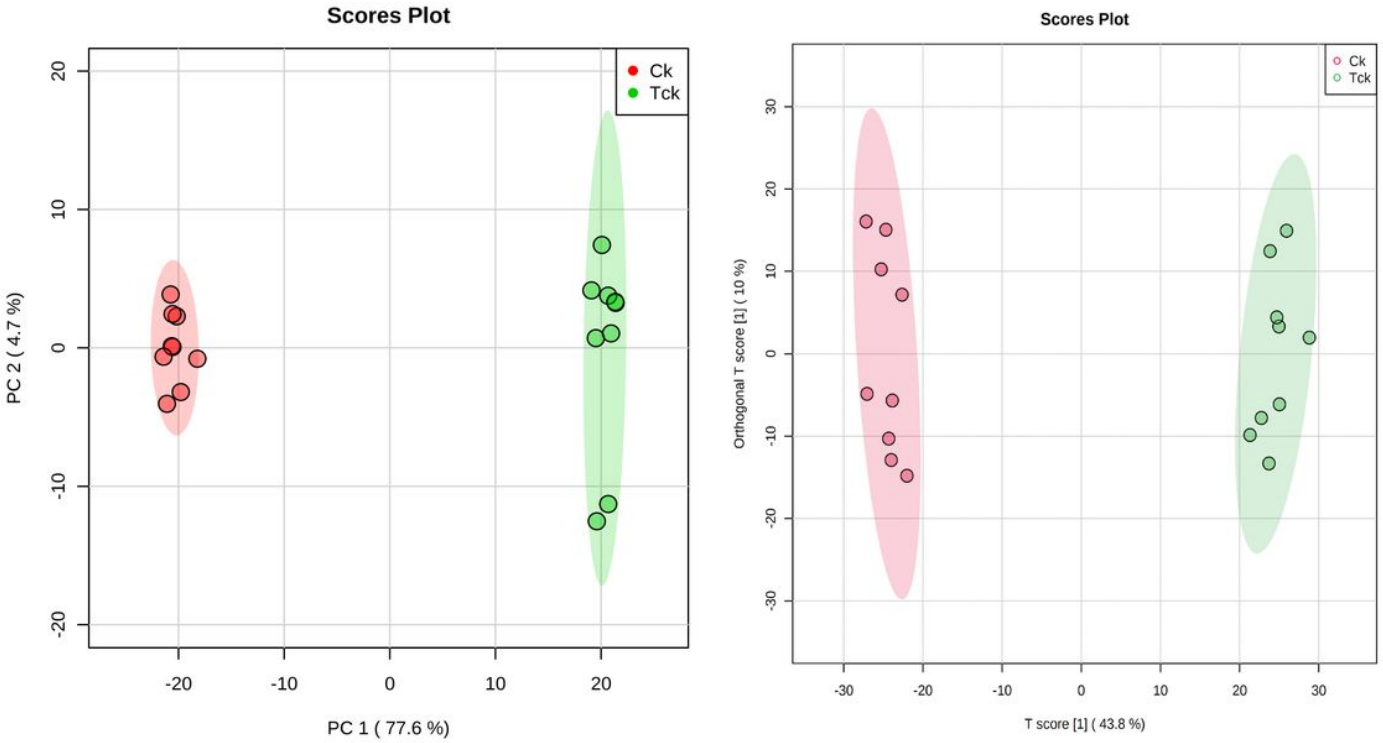

Figure 2

PCA and OPLS-DA analysis of T. controversa infected and non-infected samples. a PCA analysis for T. controversa infected and non-infected samples. b OPLS-DA analysis (=0.938). Ck stands for non-infected sample while Tck stands for T. controversa infected samples.

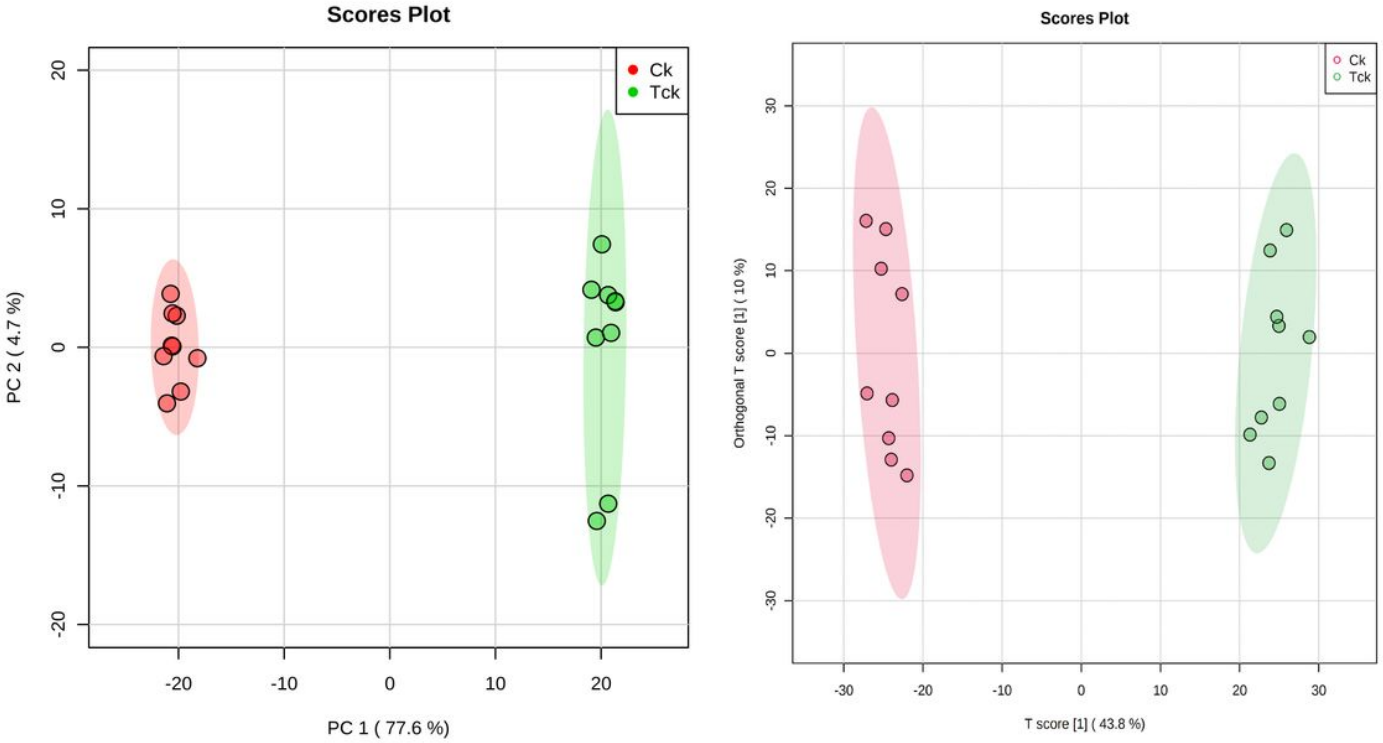

Figure 2

PCA and OPLS-DA analysis of T. controversa infected and non-infected samples. a PCA analysis for T. controversa infected and non-infected samples. b OPLS-DA analysis (=0.938). Ck stands for non-infected sample while Tck stands for T. controversa infected samples.

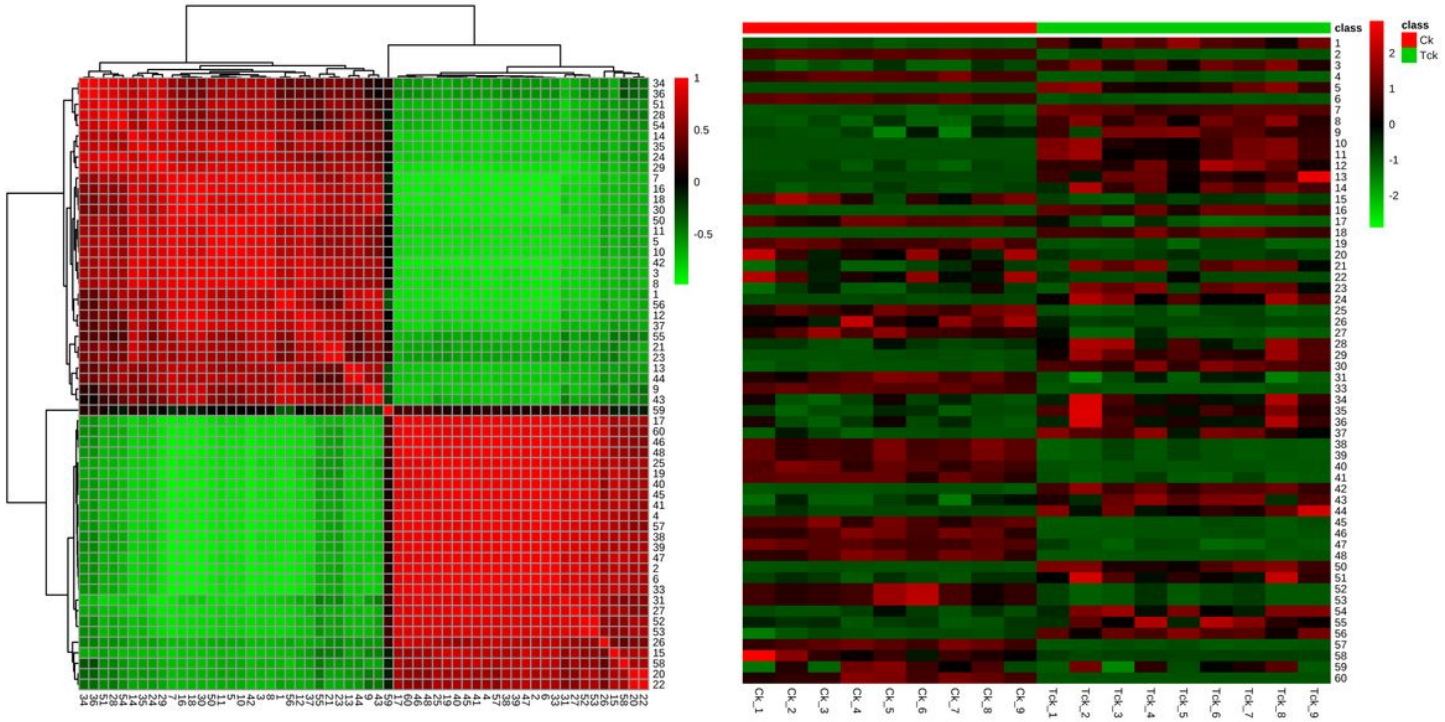

Figure 3

The hierarchical clustering heatmap visualizing the changes in the contents of potential metabolites in T. controversa infected and non-infected samples. a correlation analysis of different metabolites. Deeper color had strong correlation and lighter color had weak correlation. b hierarchical cluster analysis of different metabolites. Red color showed that metabolites increased and blue color showed that metabolites decreased.

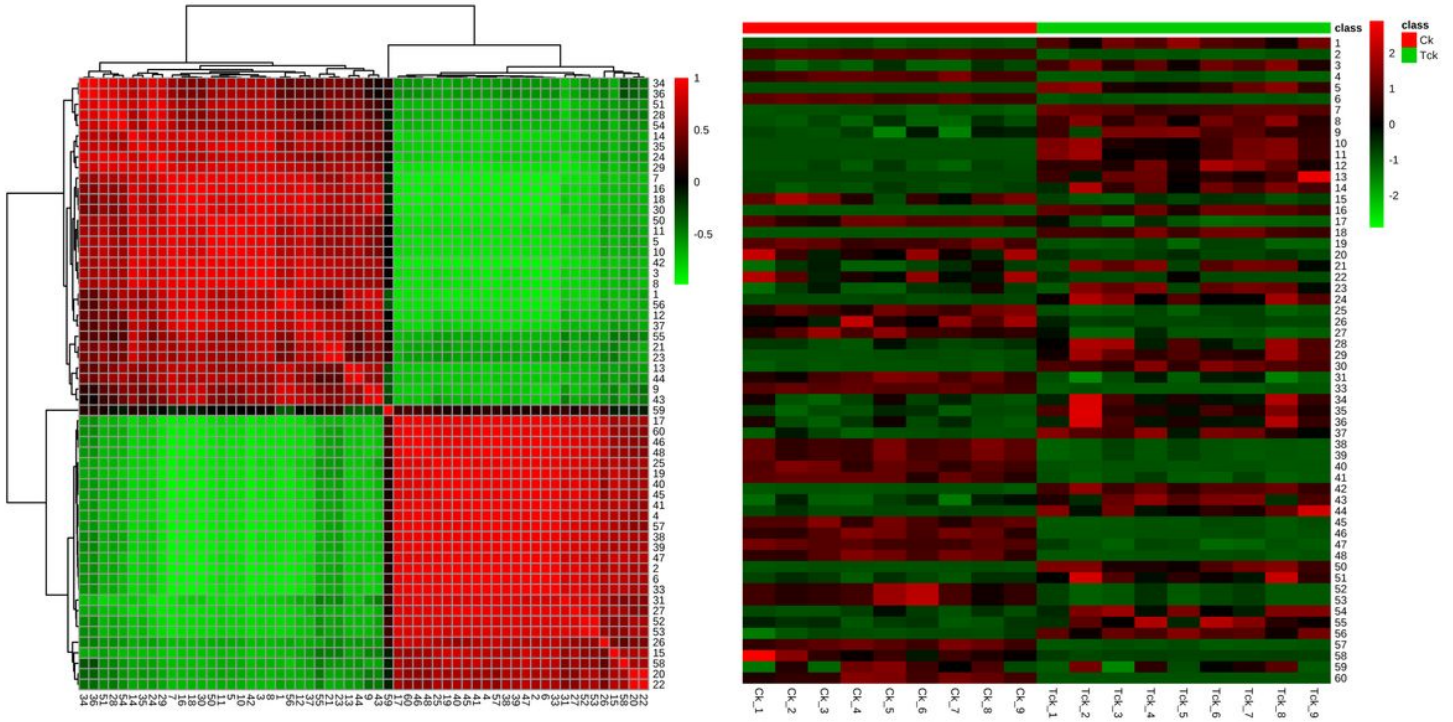

Figure 3

The hierarchical clustering heatmap visualizing the changes in the contents of potential metabolites in T. controversa infected and non-infected samples. a correlation analysis of different metabolites. Deeper color had strong correlation and lighter color had weak correlation. b hierarchical cluster analysis of different metabolites. Red color showed that metabolites increased and blue color showed that metabolites decreased.

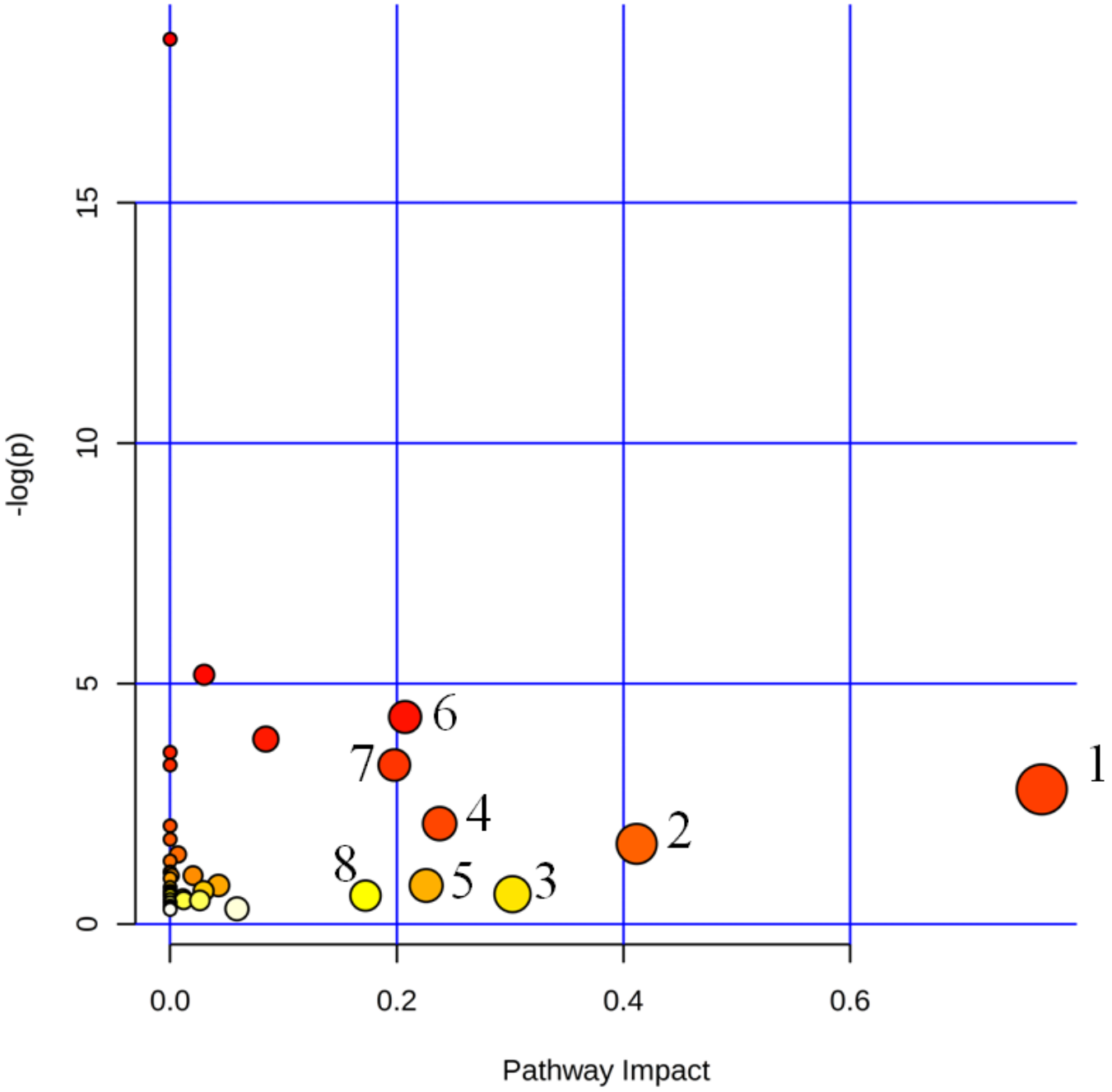

Figure 4

Pathways analysis overview showing altered metabolic pathways in T. controversa infected and non-infected samples. 1 phenylalanine metabolism; 2 isoquinoline alkaloid biosynthesis; 3 starch and sucrose metabolism; 4 tyrosine metabolism; 5 sphingolipid metabolism; 6 Arginine and proline metabolism; 7 alanine, aspartate and glutamate metabolism; 8 tryptophan metabolism. A pathway with the impact value higher than 0.1, was considered as a potential target.

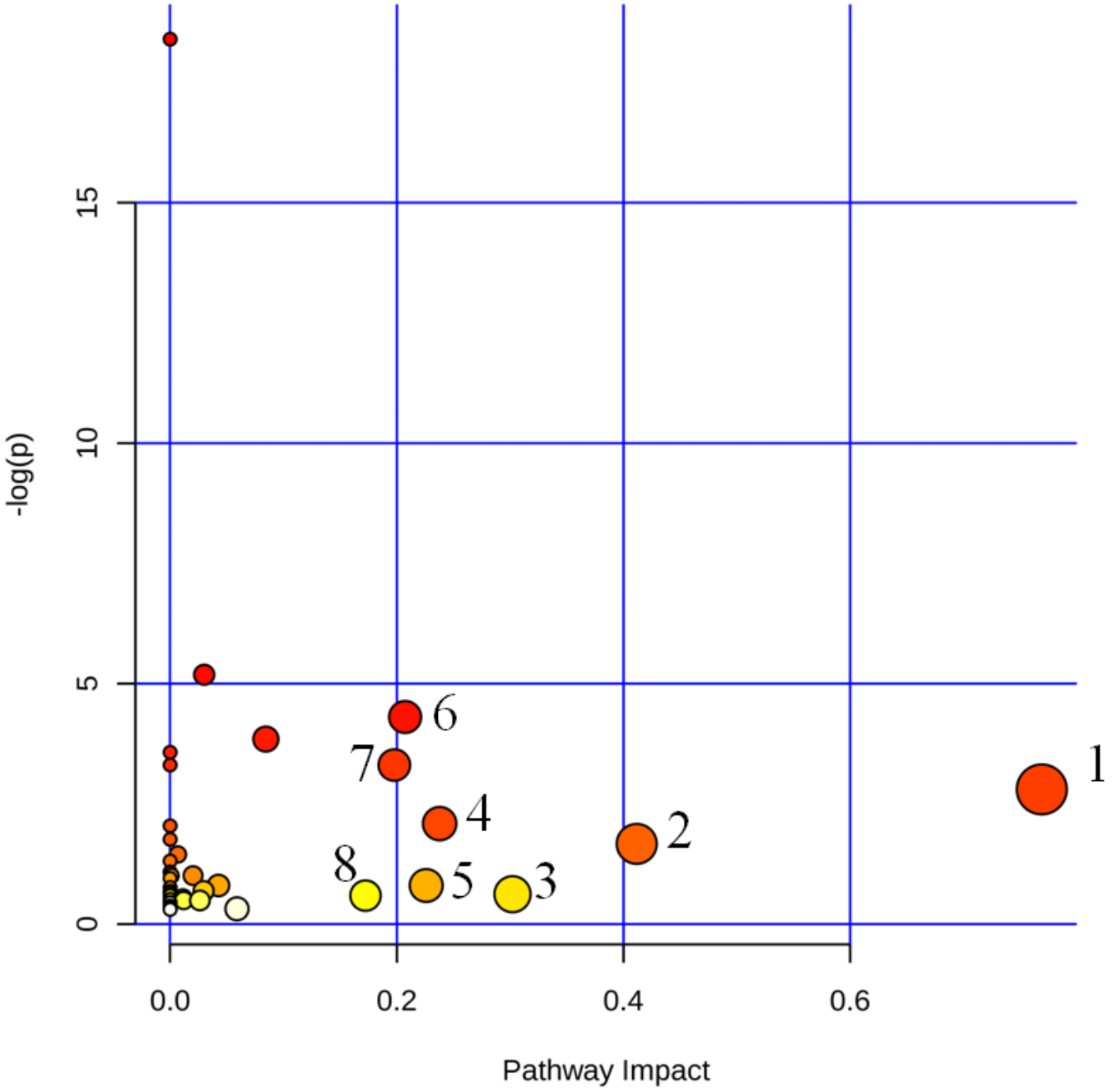

Figure 4

Pathways analysis overview showing altered metabolic pathways in T. controversa infected and non-infected samples. 1 phenylalanine metabolism; 2 isoquinoline alkaloid biosynthesis; 3 starch and sucrose metabolism; 4 tyrosine metabolism; 5 sphingolipid metabolism; 6 Arginine and proline metabolism; 7 alanine, aspartate and glutamate metabolism; 8 tryptophan metabolism. A pathway with the impact value higher than 0.1, was considered as a potential target.

Supplementary Files

This is a list of supplementary files associated with this preprint. Click to download.

- Fig.S1.png
- Fig.S1.png
- Supplementarymaterial.docx
- Supplementarymaterial.docx